

# Noncovalent Modification of Carbon Nanotubes with Pyrene-Functionalized Nickel Complexes: Carbon Monoxide Tolerant Catalysts for Hydrogen Evolution and Uptake\*\*

Phong D. Tran, Alan Le Goff, Jonathan Heidkamp, Bruno Joussetme,\* Nicolas Guillet, Serge Palacin, Holger Dau, Marc Fontecave, and Vincent Artero\*

Hydrogen production through the reduction of water appears to be a very attractive solution for the long-term storage of renewable energy. However, economically viable processes require platinum-free catalysts, since this expensive and scarce metal is not a sustainable resource.<sup>[1]</sup> We recently showed that the combination of a bioinspired molecular approach with nanochemical tools, through the covalent attachment of mimics<sup>[2,3]</sup> of the active site of hydrogenase enzymes onto carbon nanotubes (CNTs), results in a noble-metal-free electrocatalytic nanomaterial with low overpotential and exceptional stability for H<sub>2</sub> evolution or uptake.<sup>[4,5]</sup> In this initial study, we used the electroreduction of a diazonium salt to decorate multiwalled carbon nanotubes (MWCNTs) deposited on the electrode support with a polyphenylene layer bearing amino groups.<sup>[6]</sup> These amino groups were then used to attach an activated ester derivative [Ni(P<sup>Ph</sup><sub>2</sub>N<sup>Ar</sup><sub>2</sub>)<sub>2</sub>]<sup>2+</sup> of the nickel bisdiphosphine bioinspired catalyst developed

by DuBois and co-workers through the formation of an amide linkage. However, as current manufacturing techniques for active layers for fuel cells or electrolyzers rely on standard deposition or printing of an ink containing the electroactive material, this three-step procedure has obvious practical and technical drawbacks. We thus turned toward a more direct and smoother method involving noncovalent π–π stacking interactions for the functionalization of MWCNTs, since this methodology<sup>[7]</sup> has recently been shown to result into efficient electronic communication between CNTs and immobilized metal coordination complexes.<sup>[8]</sup> This approach allows straightforward and highly convenient preparation of very stable electrocatalytic materials for H<sub>2</sub> evolution and uptake with tunable catalyst loading. In addition, the catalytic activity for H<sub>2</sub> uptake displayed by this novel molecular engineered electrocatalytic material is sustained in the presence of carbon monoxide (CO), a major impurity in H<sub>2</sub> fuels derived from reformed hydrocarbons or biomass. This improvement constitutes a major breakthrough for nafion-based proton-exchange membrane (PEM) fuel cells technology, since CO poisoning limits the commercialization of devices based on Pt electrocatalysts.<sup>[9]</sup>

Condensation of pyren-1-yl methylamine with formaldehyde in the presence of phenyl- or cyclohexylphosphine yields 1,5-di(pyren-1-ylmethyl)-3,7-diphenyl-1,5-diaza-3,7-diphosphacyclooctane (P<sup>Ph</sup><sub>2</sub>N<sub>2</sub><sup>CH<sub>2</sub>Pyrene</sup>) and 1,5-di(pyren-1-ylmethyl)-3,7-dicyclohexyl-1,5-diaza-3,7-diphosphacyclooctane (P<sup>Cy</sup><sub>2</sub>N<sub>2</sub><sup>CH<sub>2</sub>Pyrene</sup>) ligands, respectively.<sup>[10]</sup> The corresponding orange-to-red nickel(II) complexes [Ni(P<sup>Ph</sup><sub>2</sub>N<sub>2</sub><sup>CH<sub>2</sub>Pyrene</sup>)<sub>2</sub>](BF<sub>4</sub>)<sub>2</sub> (**1**(BF<sub>4</sub>)<sub>2</sub>) and [Ni(P<sup>Cy</sup><sub>2</sub>N<sub>2</sub><sup>CH<sub>2</sub>Pyrene</sup>)<sub>2</sub>](BF<sub>4</sub>)<sub>2</sub> (**2**(BF<sub>4</sub>)<sub>2</sub>) are air- and moisture-stable in the solid state, and their acetonitrile solutions can be handled in air for more than 24 h without degradation, as evidenced by <sup>31</sup>P NMR measurements.

[\*] Dr. P. D. Tran, Prof. M. Fontecave, Dr. V. Artero  
 Laboratoire de Chimie et Biologie des Métaux  
 Université Joseph Fourier, CNRS UMR 5249, CEA DSV/iRTSV  
 17 rue des Martyrs, 38054 Grenoble cedex 9 (France)  
 E-mail: vincent.artero@cea.fr

Dr. A. Le Goff, Dr. B. Joussetme, Dr. S. Palacin  
 CEA, IRAMIS, SPCSI, Chemistry of Surfaces and Interfaces Group  
 91191 Gif sur Yvette Cedex (France)  
 E-mail: bruno.joussetme@cea.fr

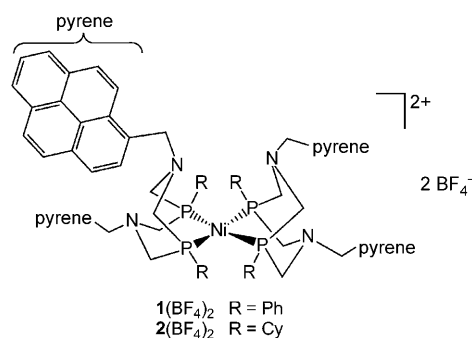
J. Heidkamp, Prof. H. Dau  
 FB Physik, Free University Berlin  
 Arnimallee 14, 14195 Berlin (Germany)

Dr. N. Guillet  
 Institut LITEN, CEA LITEN/DTH/LCPEM  
 17 rue des Martyrs, 38054 Grenoble cedex 9 (France)

Prof. M. Fontecave  
 Collège de France  
 11 place Marcellin-Berthelot, 75005 Paris (France)

[\*\*] This work was supported by the CEA (Nanosciences program, grant Grafthydro) and the ANR (PAN-H 2008, EnzHyd). The X-ray absorption experiments were supported by Dr. F Schäfers at Helmholtz Zentrum Berlin (HZB/BESSY) and by the Berlin cluster of excellence on Unifying Concepts in Catalysis (UniCat). We thank A. Fihri and J. Fize for experimental contributions and P. Jegou for XPS measurements.

Supporting information for this article (experimental details including synthetic and catalytic assay procedures, cyclic voltammograms of **1**(BF<sub>4</sub>)<sub>2</sub>, **2**(BF<sub>4</sub>)<sub>2</sub>, and [Ni(CH<sub>3</sub>CN)<sub>6</sub>](BF<sub>4</sub>)<sub>2</sub>, XPS, XANES, and EXAFS of functionalized MWCNTs/GDL, and electrocatalytic behavior of bulk catalysts and the derived materials) is available on the WWW under <http://dx.doi.org/10.1002/anie.201005427>.



Both **1**(BF<sub>4</sub>)<sub>2</sub> and **2**(BF<sub>4</sub>)<sub>2</sub> are electroactive for catalytic H<sub>2</sub> evolution from protonated *N,N*-dimethylformamide ([DMFH]OTf) in CH<sub>3</sub>CN with similar catalytic rates,<sup>[10]</sup> and the overpotential of 0.1 V is slightly lower than that displayed by the previously reported [Ni(P<sup>Ph</sup><sub>2</sub>N<sup>Ph</sup><sub>2</sub>)<sub>2</sub>](BF<sub>4</sub>)<sub>2</sub> complex,<sup>[11]</sup> probably because of the distinct nature of the nitrogen substituent. As both catalysts are unstable in CH<sub>3</sub>CN solution in the presence of Et<sub>3</sub>N, we were unable to measure their activity for H<sub>2</sub> oxidation using the electrochemical assay procedure previously described by DuBois and co-workers.<sup>[11,12]</sup> We then turned to a homogeneous assay, adapted from the conventional procedure used to determine the specific activity of native hydrogenase enzymes.<sup>[13]</sup> Both **1**(BF<sub>4</sub>)<sub>2</sub> and **2**(BF<sub>4</sub>)<sub>2</sub> proved to be active for catalytic H<sub>2</sub> (10<sup>5</sup> Pa) oxidation in CH<sub>3</sub>CN in the presence of 2,6-lutidine (2,6-Lut) [Eq. (1)] when methyl viologen hexafluorophosphate ([MV](PF<sub>6</sub>)<sub>2</sub>) was used as the electron acceptor.<sup>[10]</sup>



Catalysts **1**(BF<sub>4</sub>)<sub>2</sub> and **2**(BF<sub>4</sub>)<sub>2</sub> can be physisorbed on MWCNTs deposited on an electrode substrate through the establishment of  $\pi$ - $\pi$  stacking interactions between the pyrene moieties and graphene motifs. In a first step, MWCNTs were deposited by filtration onto commercial gas diffusion layers (GDL), developed for proton exchange membrane (PEM) applications and consisting of a carbon fiber cloth coated with a microporous teflon layer embedding carbon black so as to retain electronic conductivity properties. Scanning electron micrographs show the high specific surface displayed by the resulting electrode thanks to the formation of bundles of MWCNTs with extensive branching.<sup>[10]</sup> Secondly, a millimolar solution of catalyst **1**(BF<sub>4</sub>)<sub>2</sub> or **2**(BF<sub>4</sub>)<sub>2</sub> in CH<sub>2</sub>Cl<sub>2</sub> was slowly filtered through these MWCNTs/GDL electrodes. The electrode was then washed with CH<sub>3</sub>CN, so as to eliminate any unbound nickel complexes, and air-dried.

X-ray photoelectron spectroscopy (XPS) analysis of the Ni-functionalized MWCNTs/GDL electrodes shows on the survey spectrum the presence of Ni, P, N, B, and F constitutive elements of complex **1**(BF<sub>4</sub>)<sub>2</sub> and of oxygen from alcohol or carboxylic defects of pristine MWCNTs.<sup>[10]</sup> The decomposition of the expanded P 2p region shows four peaks: the first two peaks centered at 132.8 and 133.6 eV correspond to the P<sub>2p3/2</sub> and P<sub>2p1/2</sub> peaks, respectively, of the metal-bound phosphorous atoms<sup>[14]</sup> and the other peaks at 131.6 and 132.4 eV are attributed to P<sub>2p</sub> peaks of uncoordinated phosphine ligands adsorbed on MWCNTs. Fitting and integration of these peaks gave a ratio of 4:1. The Ni 2p<sub>3/2</sub> region is centered at 856.76 eV, which is in good agreement with the presence of a Ni<sup>II</sup> ion.

We detected a Ni K-edge position indicative of Ni<sup>II</sup> in the X-ray absorption spectrum. However, grafting **1**(BF<sub>4</sub>)<sub>2</sub> on MWCNTs modifies the X-ray absorption near-edge structure (XANES) pronouncedly.<sup>[10]</sup> The XANES spectrum is well reproduced by a weighted addition of spectra collected for **1**(BF<sub>4</sub>)<sub>2</sub> before grafting and for a Ni<sup>II</sup> coordinated to six light atoms (O, N, C), as found in [Ni(H<sub>2</sub>O)<sub>6</sub>]<sup>2+</sup> used as a model.<sup>[10]</sup> The weighting coefficients suggest that (65 ± 15)% of the Ni ions are bound to the unmodified ligand system of **1**(BF<sub>4</sub>)<sub>2</sub>,

whereas (35 ± 15)% are octahedrally coordinated by light atoms. In the latter species, nickel may be coordinated by water molecules, carboxylate, or hydroxo defects present at the surface of MWCNTs or by an oxidized diphosphine ligand, either through the phosphine oxide function or through the amine function, as shown recently in a similar system.<sup>[15]</sup> The extended X-ray absorption fine-structure (EXAFS)<sup>[10]</sup> of grafted **1**(BF<sub>4</sub>)<sub>2</sub> confirms our conclusion derived from XANES, namely, the prevalence of the Ni<sup>II</sup>P<sub>4</sub> coordination of **1**(BF<sub>4</sub>)<sub>2</sub> and presence of Ni<sup>II</sup>(O/C/N)<sub>6</sub> coordination for about one third of the Ni ions. A mixed-ligand environment of light atoms and phosphorous both coordinated to the same Ni<sup>II</sup> ion is unlikely.<sup>[10]</sup>

The cyclic voltammogram recorded in pure electrolyte (CH<sub>3</sub>CN, 0.1 mol L<sup>-1</sup> *n*Bu<sub>4</sub>NBF<sub>4</sub>) at the MWCNTs/GDL (MWCNTs loading of 0.05 mg cm<sup>-2</sup>) electrode modified with **2**(BF<sub>4</sub>)<sub>2</sub> displays two one-electron quasi-reversible systems at -0.25 (Δ*E*<sub>p</sub> = 72 mV for a scan rate of 50 mV s<sup>-1</sup>) and -0.60 V versus NHE (Δ*E*<sub>p</sub> = 68 mV; 50 mV s<sup>-1</sup>).<sup>[10]</sup> The intensities of both anodic and cathodic peaks are directly proportional to the scan rate, thus confirming the immobilization of the nickel complexes onto the electrode surface. The cyclic voltammogram recorded at an electrode modified with **1**(BF<sub>4</sub>)<sub>2</sub> shows only one reversible wave at -0.58 V versus NHE (Δ*E*<sub>p</sub> = 60 mV; 50 mV s<sup>-1</sup>), which is likely to be a combination of the two one-electron waves observed in solution.<sup>[16,17]</sup> Integration of the waves allows us to determine a surface concentration for both catalysts of (2 ± 0.5) × 10<sup>-9</sup> mol cm<sup>-2</sup>. Such electrochemical responses were found to be highly reproducible with distinct electrodes and do not evolve with time nor depend on storage conditions. No electrochemical signal could be attributed to the Ni species coordinated to six light atoms. Control experiments with bulk [Ni(CH<sub>3</sub>CN)<sub>6</sub>]<sup>2+</sup> show that such species display irreversible response at potentials distinct from that observed for the modified electrodes.<sup>[10]</sup> XAS studies are underway to investigate whether the degraded Ni species can be electrochemically converted back into NiP<sub>4</sub> under cycling conditions.

We then investigated H<sub>2</sub> production and uptake catalyzed by the new electrode materials with 0.5 mol L<sup>-1</sup> aqueous sulfuric acid as the electrolyte. The Ni-functionalized MWCNTs/GDL electrodes were assembled with a nafion membrane to protect the catalyst from the acidic solution while allowing protons to reach or escape the catalytic layer. These membrane electrode assemblies (MEAs) containing either **1**(BF<sub>4</sub>)<sub>2</sub> or **2**(BF<sub>4</sub>)<sub>2</sub> display electrocatalytic activities for H<sub>2</sub> evolution as well as for H<sub>2</sub> oxidation (Figure 1). Remarkably, both processes occur at vanishingly small overpotentials as shown by the fact that the traces steeply cut through the potential axis at the equilibrium potential. Chronoamperometric measurements carried out at -0.3 V versus NHE under the same conditions did not show any loss of activity after a 6 h experiment corresponding to 8.5 × 10<sup>4</sup> turnovers,<sup>[10]</sup> clearly indicating the remarkable robustness of this catalytic material and consistent with the lack of any leaching of the  $\pi$ -stacked catalysts. The material obtained from **2**(BF<sub>4</sub>)<sub>2</sub> proves to be slightly more efficient for H<sub>2</sub> oxidation than the material obtained from **1**(BF<sub>4</sub>)<sub>2</sub>, which is as anticipated from the solution study.<sup>[10]</sup>

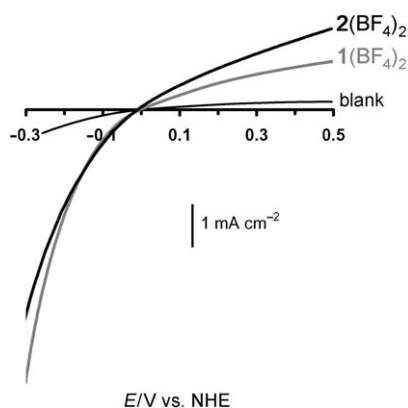


**Figure 1.** Evolution of current density as a function of potential for both H<sub>2</sub> production and uptake from a 0.5 M H<sub>2</sub>SO<sub>4</sub> aqueous solution under an atmosphere of H<sub>2</sub> (10<sup>5</sup> Pa, H<sub>2</sub> flux rate = 20 sccm), recorded at an MEA consisting of a gas diffusion layer (GDL) assembled with a nafion membrane (2 mV s<sup>-1</sup>): — unfunctionalized MWCNT/GDL; — MWCNT/GDL functionalized through  $\pi$ -stacking of **1**(BF<sub>4</sub>)<sub>2</sub> (surface catalyst concentration  $(2 \pm 0.5) \times 10^{-9}$  mol<sub>Ni</sub> cm<sup>-2</sup>); — MWCNT/GDL functionalized through  $\pi$ -stacking of **2**(BF<sub>4</sub>)<sub>2</sub> (surface catalyst concentration  $(2 \pm 0.5) \times 10^{-9}$  mol<sub>Ni</sub> cm<sup>-2</sup>).

As a major drawback, the previously used electrografting procedure imposes some limitation on the amount of grafted catalysts, since the growth of the polyphenylene layer partially fills the pores of the MWCNTs deposit, thus leading to degradation of the electron- and mass-transport performances. As a consequence, we were not able to increase the surface concentration above  $(1.5 \pm 0.5) \times 10^{-9}$  mol<sub>Ni</sub> cm<sup>-2</sup>, regardless of the amount of CNTs deposited on the GDL, and the current densities above a few mA cm<sup>-2</sup>.<sup>[4]</sup> By contrast, the  $\pi$ -stacking methodology reported herein allows decoration of the MWCNTs with a monolayer of catalysts so that catalyst loading on MWCNTs/GDL electrodes can be easily tuned by controlling the amount of CNTs initially deposited on the GDL electrode. Thus, surface catalyst concentrations can be linearly increased up to  $(1.1 \pm 1) \times 10^{-8}$  mol<sub>Ni</sub> cm<sup>-2</sup> for CNT loading of 0.3 mg cm<sup>-2</sup>.<sup>[10]</sup> Catalytic current density for H<sub>2</sub> evolution linearly increases with catalyst loading to reach almost 20 mA cm<sup>-2</sup> (Figure 2). Current densities for H<sub>2</sub> oxidation increased much less. Moreover, the two new materials display catalytic current densities for H<sub>2</sub> oxidation comparable to those generated by the previously reported one,<sup>[4]</sup> in which the nickel catalyst was covalently grafted.<sup>[10]</sup> Given the contrasting catalytic performances of bulk (ungrafted) **1**(BF<sub>4</sub>)<sub>2</sub>, **2**(BF<sub>4</sub>)<sub>2</sub>, and [Ni(P<sup>Ph</sup><sub>2</sub>N<sup>Ar</sup><sub>2</sub>)<sub>2</sub>]<sup>2+</sup> (Ar = aryl) for H<sub>2</sub> evolution,<sup>[10]</sup> these observations indicate that mass transport of H<sub>2</sub> gas within a film of functionalized CNTs limits the catalytic rates and thus the anodic current density.

A very important limitation of the use of platinum nanoparticles as electrocatalysts for H<sub>2</sub> oxidation in fuel cells comes from the poisoning effect of CO.<sup>[9]</sup> Hence, we investigated the catalytic performances of Ni-functionalized materials for H<sub>2</sub> (10<sup>5</sup> Pa) oxidation in the presence of CO (50 ppm) and found no inhibiting effect of this pollutant (Figure 3 and the Supporting Information). Solution studies have shown that binding of CO to nickel(II) bisdiphosphine

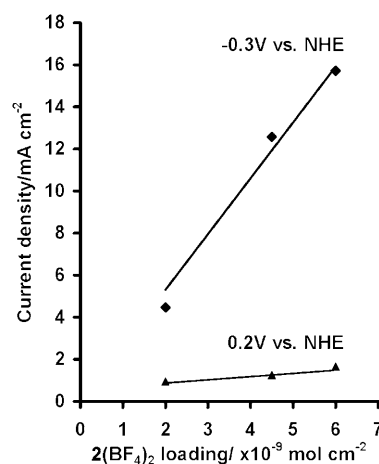


**Figure 2.** Evolution of the current densities for H<sub>2</sub> evolution (-0.3 V vs. NHE) and uptake (0.2 V vs. NHE) as a function of the surface catalyst concentration in MEA obtained from **2**(BF<sub>4</sub>)<sub>2</sub>.

complexes is either ineffective or reversible without inhibiting H<sub>2</sub>-oxidation catalysis.<sup>[11,18]</sup> Nicely, this property is retained in the materials after grafting. For comparison, commercial MEAs containing highly dispersed platinum (0.5 mgPt cm<sup>-2</sup>) are rapidly and completely deactivated over minutes under the same conditions (Figure 3).

The  $\pi$ - $\pi$  stacking functionalization of MWCNTs with bioinspired molecular complexes thus appears to be a straightforward methodology to prepare highly robust, CO-tolerant, noble-metal-free, and bidirectional electrocatalytic nanomaterials for H<sub>2</sub> evolution and uptake, which are compatible with the conditions encountered in classical proton-exchange membrane devices. The materials reported herein can be prepared in one step from MWCNTs and pyrene-functionalized complexes and then deposited onto any electrode support. A major challenge will now consist of

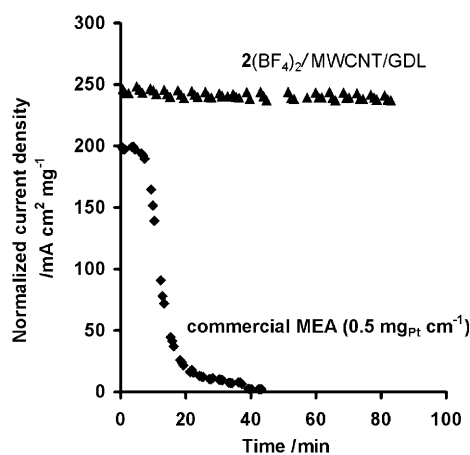


**Figure 3.** Evolution upon repeated cycling (2 mV s<sup>-1</sup>) of the H<sub>2</sub> oxidation current density per mg of deposited catalyst recorded at 0.25 V versus NHE for a nickel-functionalized MWCNT/GDL electrode (prepared from **2**(BF<sub>4</sub>)<sub>2</sub>; surface catalyst concentration:  $(2 \pm 0.5) \times 10^{-9}$  mol cm<sup>-2</sup>) and a commercial Pt-based active layer (Pt nanoparticles deposited on carbon black, 0.5 mg<sub>Pt</sub> cm<sup>-2</sup>) under an atmosphere of H<sub>2</sub> polluted with 50 ppm CO (flux rate: 20 sccm).

significantly improving the catalytic loading so as to reach the power performances displayed by commercial Pt-based active layers. To this end, again the  $\pi$ - $\pi$  stacking methodology allows such tuning of the catalytic loading by increasing the amount of supporting MWCNTs. Since specific  $\text{H}_2$  oxidation current densities (i.e. relative to the mass of immobilized catalyst including metal, ligands, and counteranions, if applicable, as shown in Figure 3) obtained with the Ni-based materials ( $250 \text{ mA cm}^{-2} \text{ mg}_{\text{catalyst}}^{-1}$  for  $\mathbf{2}(\text{BF}_4)_2$ ) and with commercial active layers containing highly dispersed platinum ( $200 \text{ mA cm}^{-2} \text{ mg}_{\text{Pt}}^{-1}$ ;  $0.5 \text{ mg}_{\text{Pt}} \text{ cm}^{-2}$ ) are comparable, this methodology paves the way for the implementation of noble-metal-free electrocatalytic materials in operative PEM devices.

Received: August 30, 2010

Published online: January 5, 2011

**Keywords:** carbon · heterogeneous catalysis · hydrogen · nanotubes · nickel

- 
- [1] R. B. Gordon, M. Bertram, T. E. Graedel, *Proc. Natl. Acad. Sci. USA* **2006**, *103*, 1209–1214.
- [2] S. Canaguier, V. Artero, M. Fontecave, *Dalton Trans.* **2008**, 315–325.
- [3] C. Tard, C. J. Pickett, *Chem. Rev.* **2009**, *109*, 2245–2274.
- [4] A. Le Goff, V. Artero, B. Jusselme, P. D. Tran, N. Guillet, R. Metaye, A. Fihri, S. Palacin, M. Fontecave, *Science* **2009**, *326*, 1384–1387.
- [5] P. D. Tran, V. Artero, M. Fontecave, *Energy Environ. Sci.* **2010**, *3*, 727–747.
- [6] A. Le Goff, F. Moggia, N. Debou, P. Jegou, V. Artero, M. Fontecave, B. Jusselme, S. Palacin, *J. Electroanal. Chem.* **2010**, *641*, 57–63.
- [7] Y. L. Zhao, J. F. Stoddart, *Acc. Chem. Res.* **2009**, *42*, 1161–1171.
- [8] E. W. McQueen, J. I. Goldsmith, *J. Am. Chem. Soc.* **2009**, *131*, 17554–17556.
- [9] J. J. Baschuk, X. G. Li, *Int. J. Energy Res.* **2001**, *25*, 695–713.
- [10] See the Supporting Information.
- [11] A. D. Wilson, R. H. Newell, M. J. McNevin, J. T. Muckerman, M. R. DuBois, D. L. DuBois, *J. Am. Chem. Soc.* **2006**, *128*, 358–366.
- [12] J. Y. Yang, R. M. Bullock, W. J. Shaw, B. Twamley, K. Frazee, M. R. DuBois, D. L. DuBois, *J. Am. Chem. Soc.* **2009**, *131*, 5935–5945.
- [13] V. Artero, M. Fontecave, *Coord. Chem. Rev.* **2005**, *249*, 1518–1535.
- [14] The signal of oxidized phosphine ligand, either coordinated or not, would appear at the same energy.
- [15] J. Y. Yang, R. M. Bullock, W. G. Dougherty, W. S. Kassel, B. Twamley, D. L. DuBois, M. R. DuBois, *Dalton Trans.* **2010**, 39, 3001–3010.
- [16] Actually, the two  $\text{Ni}^{\text{II/I}}$  and  $\text{Ni}^{\text{I/0}}$  redox features are quite narrow in  $\mathbf{1}(\text{BF}_4)_2$  and  $[\text{Ni}(\text{P}^{\text{Ph}}_2\text{N}^{\text{Ph}}_2)_2](\text{BF}_4)_2$  relative to that of  $\mathbf{2}(\text{BF}_4)_2$ . Such behavior has been traced to structural distortions.<sup>[19]</sup>
- [17] G. M. Jacobsen, J. Y. Yang, B. Twamley, A. D. Wilson, R. M. Bullock, M. R. DuBois, D. L. DuBois, *Energy Environ. Sci.* **2008**, *1*, 167–174.
- [18] A. D. Wilson, K. Frazee, B. Twamley, S. M. Miller, D. L. DuBois, M. R. DuBois, *J. Am. Chem. Soc.* **2008**, *130*, 1061–1068.
- [19] J. W. Raebiger, A. Miedaner, C. J. Curtis, S. M. Miller, O. P. Anderson, D. L. DuBois, *J. Am. Chem. Soc.* **2004**, *126*, 5502–5514.
-